IEEE Access
Multidisciplinary | Rapid Review | Open Access Journal

Received August 5, 2020, accepted September 23, 2020, date of publication October 5, 2020, date of current version October 15, 2020.

Digital Object Identifier 10.1109/ACCESS.2020.3028570

Optimal Parameter Design by NSGA-II and Taguchi Method for RCD Snubber Circuit

YING MA[1], FU-I CHOU[2], PO-YUAN YANG[3], JINN-TSONG TSAI[4], ZHEN-YU YANG[5], AND JYH-HORNG CHOU[5,6,7], (Fellow, IEEE)

[1]School of Information Science and Engineering, Fujian University of Technology, Fuzhou 350118, China
[2]Department of Automation Engineering, National Formosa University, Huwei 63201, Taiwan
[3]Department of Information Engineering and Computer Science, Feng Chia University, Taichung 40724, Taiwan
[4]Department of Computer Science, National Pingtung University, Pingtung 900391, Taiwan
[5]Department of Electrical Engineering, National Kaohsiung University of Science and Technology, Kaohsiung 80778, Taiwan
[6]Department of Mechanical Engineering, National Chung-Hsing University, Taichung 40227, Taiwan
[7]Department of Healthcare Administration and Medical Informatics, Kaohsiung Medical University, Kaohsiung 80708, Taiwan

Corresponding authors: Po-Yuan Yang (pyang@fcu.edu.tw), Jinn-Tsong Tsai (jttsai@mail.nptu.edu.tw), and Jyh-Horng Chou (choujh@nkust.edu.tw)

This work was supported in part by the Ministry of Science and Technology, Taiwan, Republic of China, under Grant MOST 107-2221-E-992-086-MY3, Grant MOST 109-2222-E-150-002-MY2, Grant MOST 109-2222-E-035-002, and Grant MOST 109-2221-E-153-005-MY3; and in part by the Intelligent Manufacturing Research Center (iMRC) from the Featured Areas Research Center Program within the framework of the Higher Education Sprout Project, Ministry of Education (MOE), Taiwan.

ABSTRACT A genetic algorithm and Taguchi method were used to optimize parameters for the residual-current device (RCD) snubber circuit of a DC-DC flyback converter. The most suitable algorithm was determined by using test functions to compare performance in three multi-objective optimization methods: non-dominated sort genetic algorithm-II (NSGA-II), multi-objective particle swarm optimization (MOPSO), and multi-objective differential evolution algorithm (MODE). Comparisons of coverage rate, distance between non-dominant solutions, and maximum walking distance showed that NSGA-II was superior to both MOPSO and MODE. Therefore, NSGA-II was used to obtain parameter values for the RCD snubber circuit. However, practical application of the parameter values was limited because the values could not meet the specifications required for real-world circuits. Thus, the parameter values obtained by NSGA-II were used in further factor-level experiments performed by Taguchi method. The experimental results indicated that, compared to previous design methods, the proposed NSGA-II and Taguchi method obtains better parameter values for the RCD snubber circuit.

INDEX TERMS Multi-objective optimization, Taguchi method, RCD snubber circuit.

I. INTRODUCTION

The residual-current device (RCD) snubber is usually used in flyback converter, in order to limit the voltage spikes caused by leakage inductance of the transformer [1]–[3]. This converter is an essential power electronics product that is widely used in many industries, including manufacturing, medicine, aerospace, and the defense. The stable, high quality power supplied from this converter directly enhances performance and safety in many electronic products. Therefore, how to select the proper snubber circuit and obtain the optimal design is an issue worth investigating [4], [5]. Sun *et al.* [4] proposed an improved genetic algorithm to optimize the design of AC-DC converter with snubber in switching power amplifier. Huang *et al.* [5] gave a single-objective optimal design method of DC-DC converter with an RCD snubber by using a genetic algorithm and the Taguchi method. An economical, practical, and efficient circuit design procedure is provided by Huang *et al.* [5], [6]. However, Huang *et al.* [5] only considered the single-objective problem of reducing the spike voltage. Reducing energy loss on the RCD snubber circuit is also an issue worth investigating. However, to the authors' best knowledge, there are no literatures to studying the optimal problem of reducing both spike voltage and energy loss on the RCD snubber circuit.

As the intelligent manufacturing industry evolves, single-objective optimization methods have increasingly revealed limitations in meeting industrial demands. Therefore, multi-objective optimization has been widely used in the product design and production processes of various industries in

The associate editor coordinating the review of this manuscript and approving it for publication was Jenny Mahoney.

recent years. The main purpose of multi-objective optimization is to resolve conflicts among various objectives [7]–[10]. Multi-objective optimization methods currently used in the industry are often derived from single-objective optimization methods such as genetic algorithm (GA), particle swarm optimization (PSO) and differential evolution algorithm (DEA).

The first multi-objective optimization algorithm, vector evaluated genetic algorithm (VEGA), was proposed by Schaffer [11]. The VEGA is easy to apply but can only find the best solution for a single objective. Improvements in VEGA proposed by Hajela and Lin [12] and by Fonseca and Fleming [13] resulted in the weight-based genetic algorithm and the multi-objective genetic algorithm (MOGA), respectively. The non-dominated sorting genetic algorithm (NSGA) was introduced by Deb and Srinivas from MOGA [14] and further refined by Deb *et al.* [15]. The original NSGA had two shortcomings: it was incapable of finding the best solution, and it tended to fall into the regional solution. The second generation NSGA (NSGA-II) addressed these shortcomings by applying an elite dominated strategy [15]. The many applications of NSGA-II have included pipe routing for aviation engines [16] and electricity price prediction [17]. Coello and Lechunga [18] proposed grid-based multi-objective particle swarm optimization (MOPSO) based on grid selection. A modification of MOPSO in 2004 enhanced its search capability by considering domination and non-domination relationships and by applying perturb and observe method [19]. A notable application of MOPSO is in cloud computing [20] to maximize broker profit while minimizing time cost. Abbass *et al.* [21] proposed the Pareto differential evolution algorithm (PDEA), which applied the dominance relation in DEA. Babu and Jehan [22] proposed the use of DEA in multi-objective optimization (MODE). Kukkonen and Lampinen [23] introduced the third evolution of DEA, which increased diversity of understanding. Huang *et al.* [24] proposed the self-adaptive differential evolution algorithm and Mirjalili [25] proposed a multi-objective optimization method based on dragonfly algorithm [26]. The MODE has been used to optimize the operating point of an auxiliary power unit to reduce its emissions [25].

Nowadays, one of popular solutions for the multi-objective optimal design problem is combined experimental design method with multi-objective optimization algorithm. Le Chau *et al.* [27] combined Taguchi method with DEA to solve the multi-objective optimization problem for a leaf compliant joint for micro-positioning systems. Dao and Huang [28] integrated Taguchi method with fuzzy logic to optimize a broad self-amplified 2-DOF monolithic mechanism. Dao *et al.* [29] utilized Taguchi method to obtain ranges for parameters, and then cuckoo search algorithm find the optimal parameter values according to the ranges obtained by Taguchi method. Huang and Dao [30], and Huynh *et al.* [31] exploited Taguchi method with grey relational analysis to optimize design of a 2-DOF flexure-based mechanism and the compliant mechanism flexure hinge, respectively. The validation results from those methods dovetailed nicely with the simulations.

Since follow-up studies have not adequately addressed the multi-objective optimal design problem of RCD snubber, this study proposes a multi-objective method for simultaneous optimization of reducing both spike voltage and energy loss on the RCD snubber circuit. The proposed multi-objective optimization method has many potential applications in circuit design. The experiment in this study used a flyback converter circuit as an example to verify the proposed approach.

Because the best solution found by the meta-heuristic optimization method cannot be directly used in practical applications, to meet the real-world component configuration, the best solution found by the meta-heuristic optimization method corresponds to several numerically approximated components, and then use the Taguchi method to find the most suitable configuration of real components and produce an approximate best solution that fits the real world.

This paper is organized as follows. Section 2 introduces the experimental design of the system. Section 3 introduces the design and implementation of three common multi-objective optimization methods. Section 4 presents the procedure for using Taguchi method to optimize the parameters and the design of RCD snubber circuit hardware. Finally, Section 5 concludes the study.

II. EXPERIMENTAL DESIGN

A. INTRODUCTION OF EXPERIMENTAL OBJECTS

The flyback converter circuit has several advantages, including its low cost and simple structure. Because it can implement multiple outputs, this circuit is widely used in auxiliary power systems that supply power to the whole system. To enhance power and to meet safety standards, practical applications of converter circuit designs must isolate input and output. The flyback buck-boost converter uses a coupled inductor for energy conversion. The storage and release of magnetic energy must be considered in the overall circuit design. Since the circuit structure of the flyback converter has no vibration characteristics, electrical isolation of the circuit is not required. Figure 1 shows the basic flyback converter equivalent circuit, where V_{in} is input voltage; Q is an N channel MOSFET power switch; L_m and L_e are the transformer primary side excitation inductor and transformer primary leakage inductance, respectively; n is the transformer turn ratio; and D_o, C_o, and V_o are the output diode, output capacitor, and output voltage, respectively.

A major limitation of the basic flyback converter is that magnetic inductor L_m and leakage inductance L_e in the transformer itself. To reduce voltage spikes and ringing noise, Hren added a basic flyback converter to an RCD snubber in Hren *et al.* [32]. Adding the flyback converter not only reduces noise and ringing phenomena, it also provides an energy path for the release of leakage inductance on two sides, which is essential for sharing the cross voltage for the power switch. Figure 2 shows the loop circuit, which is also known as a soft-switched flyback converter.

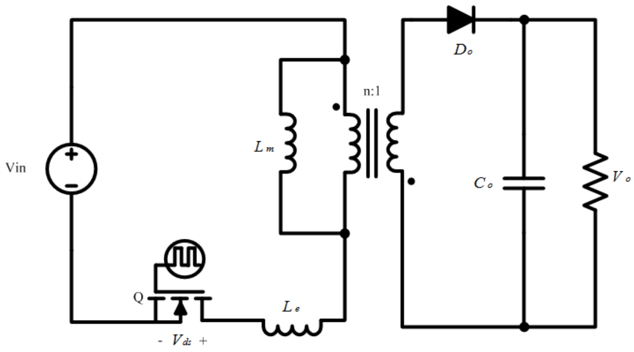

FIGURE 1. Basic flyback converter.

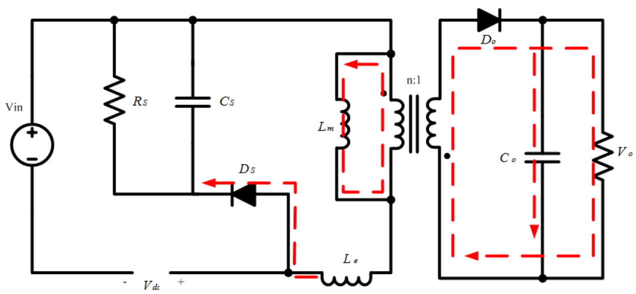

FIGURE 2. Transformer with RCD snubber.

Energy loss in the RCD snubber circuit can be divided into two stages. This study considered both stages. Stage 1 is t_1 to t. When the dipole is directed, the energy stored leakage inductance L_e is released through dipole D_s to capacitor C_s. According to the law of conservation of energy, energy loss in the circuit (W_1) can be indexed by subtracting the energy stored in the leakage inductance of transformer L_e and the energy on capacitor C_s from the energy on the transformer as shown in (2.1) below:

$$\begin{aligned} W_1 &= nV_o \int_{t_1}^{t} idt - C_s \int_{v(t_1)}^{v(t)} vdv - L_e \int_{i(t_1)}^{i(t)} idi \\ &= nV_o \cdot C_s(V_{cH} - V_{cp}) - \frac{1}{2}C_s({V_{cH}}^2 - {V_{cp}}^2) + \frac{1}{2}L_e {I_Q}^2 \end{aligned} \tag{2.1}$$

where I_Q denotes the peak voltage of the power switch, V_{cp} is the initial voltage of capacitor C_s; V_{cH} is the conduction state of the dipole. The final voltage value for capacitance C_s is defined as follows:

$$V_{cs}(t_1) = V_{cp}, \tag{2.2}$$

$$V_{ds\_pk} \cong V_{in} + V_{cp} \tag{2.3}$$

$$\ln V_{cp} - \ln V_{cH} = -\frac{T}{C_s R_s} \tag{2.4}$$

Stage 2 is t to t_1. When the energy stored in C_s is released at R_s, energy loss W_2 from resistance R_s at this time can be defined as

$$W_2 = \frac{1}{2}C_s({V_{cH}}^2 - {V_{cp}}^2) \tag{2.5}$$

The total energy loss P_{loss} on the RCD snubber circuit can be defined as

$$\begin{aligned} P_{loss} &= f_s \cdot (W_1 + W_2) \\ &= f_s \cdot \ [nV_o \cdot C_s(V_{cH} - V_{cp}) + \frac{1}{2}L_e {I_Q}^2] \end{aligned} \tag{2.6}$$

B. LOSS FUNCTION SELECTION

This study considered the optimal design of the smaller the better of two conflicting targets in the RCD snubber circuit:

(1) Reducing the peak voltage on the power switch;
(2) Reducing the energy loss on the RCD snubber circuit.

The objective functions are as follows:
Objective function 1 (peak voltage):

$$\begin{aligned} \min\ V_{ds\_pk} = V_{in} + nV_o + \Bigg(& \frac{\frac{1}{2R_sC_s} \cdot nV_o}{\sqrt{\left(\frac{1}{2R_sC_s}\right)^2 - \frac{1}{L_eC_s}}} \\ & + \frac{I_Q}{\sqrt{\left(\frac{1}{2R_sC_s}\right)^2 - \frac{1}{L_eC_s}} \cdot C_s} \Bigg) \\ & \times \exp\left(-\frac{\pi \cdot \frac{1}{2R_sC_s}}{2 \cdot \sqrt{\left(\frac{1}{2R_sC_s}\right)^2 - \frac{1}{L_eC_s}}}\right) \end{aligned} \tag{2.7}$$

Objective function 2 (total energy loss in snubber circuit):

$$\min\ P_{loss} = f_s \cdot \ [nV_o \cdot C_s(V_{cH} - V_{cp}) + \frac{1}{2}L_e {I_Q}^2] \tag{2.8}$$

C. SELECTION FOR CONTROL PARAMETERS

Based on the above objective functions analysis, the peak value of power switch V_{ds_pk} and total energy loss P_{loss} are affect by electricity leakage L_e, snubber capacitor C_s and resistance R_s. The control parameters considered in this paper are the three circuit components R_s, C_s and L_e.

The range of resistance R_s and capacitance C_s is the main consideration in ready-made products on the market, where R_s is [1 - 10] (unit: $K\Omega$), C_s is [1 - 100] (unit: nF), and L_e is [32, 43.5, 58] (unit: μH) from three self-winding transformers according to the parameters calculated in this experiment.

Figures 3 and 4 show that two objectives change with snubber resistance R_s and that two objectives change with snubber capacity C_s, respectively. Figure 3 shows that, as R_s increases, peak voltage increases but loss decreases. Figure 4 further shows that, as C_s increases, peak voltage decreases, but loss increases, however, the increase is not obvious. Figures 5-6 show how the efficiency of the converter increase with R_s and C_s, respectively.

The above discussion reveals that the optimal design must resolve the conflict between the two objectives. Therefore, this study used a multi-objective optimization method to

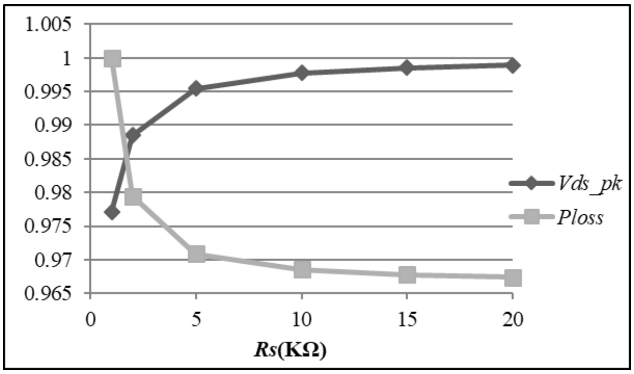

FIGURE 3. Objective changes with R_S.

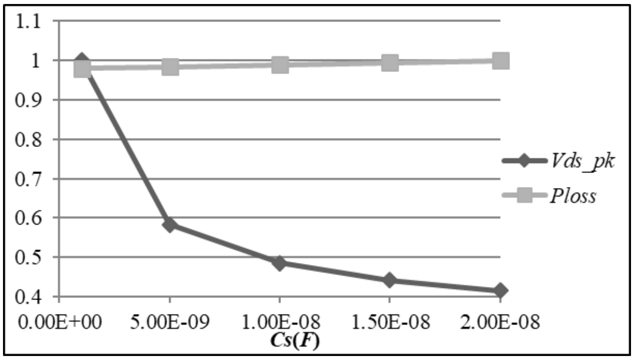

FIGURE 4. Objective changes with C_S.

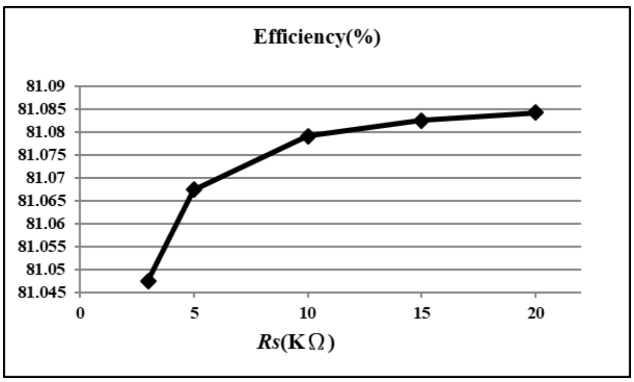

FIGURE 5. Efficiency increases with increases in R_S.

design the optimal circuit given the conflict between two targets. The effect of reducing voltage surge V_{ds_pk} and snubber loss P_{loss} on power switch Q were then determined.

D. PARAMETER SETTINGS FOR OPTIMIZATION

This study compared three multi-objective optimization methods: NSGA-II, MOPSO and MODE. Table 1 shows the parameter settings used in the comparisons. In the experiment, the three multi-objective optimization methods were used to calculate the optimal solution space when using the parameters shown in Table 1. The number of function evaluation is a critical criterion to compare optimization methods. The number of function evaluation is the number of evaluating main objective functions during iteration. In the study, the greatest number of function evaluations is 6×10^4. NSGA-II does not adopt an external storage (archive) for the Pareto optimality. Instead, each generation first performs genetic operations on the population to obtain subpopulations and then merges the two populations to perform non-inferior ranking and crowding distance ranking to obtain a new generation of populations until the end of the calculation. Therefore, there is no need to set the number of archives in NSGA-II.

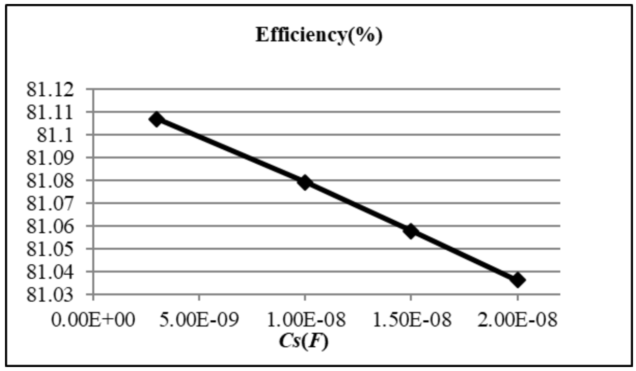

FIGURE 6. Efficiency increases with increases in C_S.

TABLE 1. Parameter settings for optimization.

Optimization	Population size	Archive	No. of generations
NSGA-II	200	X	300
MOPSO	200	200	300
MODE	200	200	300

III. DESIGN AND IMPLEMENTATION OF MULTI-OBJECTIVE OPTIMIZATION METHODS

A. NON-DOMINATED SORTING GENETIC ALGORITHM BASED ON ELITE STRATEGY (NSGA-II)

The NSGA-II was proposed by Deb and Srinivas [14] and Deb *et al.* [15]. The novel feature of NSGA-II is that non-dominated sorting and clustering are used to form several different levels of Pareto front solutions in the solution set. The NSGA-II adds the concept of crowding distance and competitive choice. The algorithm not only reduces computational complexity, it also overcomes the limitation of the original NSGA, which is its tendency to fall into regional solutions. The NSGA-II also reduces computational complexity to $O(mN^2)$. The procedure of the NSGA-II is roughly similar to that of the GA. That is, it generates offspring groups by selection, crossover, and mutation, and then performs union actions with the parents. Then, the chromosomes of offspring groups and parents are sorted by the non-dominated solution, and the crowding degree of each non-dominated level parameter is calculated. Finally, according to non-dominated relationship and crowding degree, the best chromosome is chosen to enter the next generation until the termination condition is met. Figure 7 shows a flowchart of the NSGA-II.

The crossover and mutation operations of the NSGA-II were performed by simulated binary crossover [33]

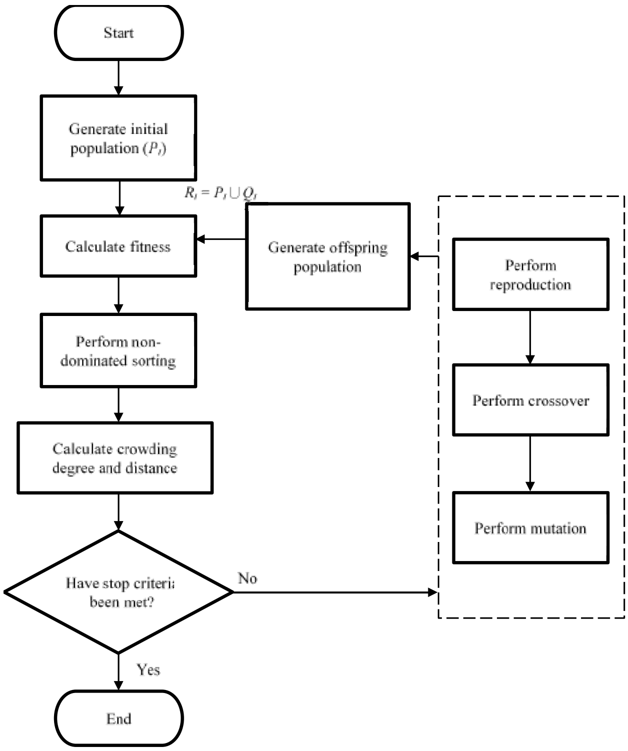

FIGURE 7. Flowchart of non-dominated sort genetic algorithm-II.

TABLE 2. Parameters and values in NSGA-II.

	R_s (Ω)	C_s (F)	L_e (H)	V_{ds_pk} (V)	P_{loss} (W)
1	1038.304	1.00×10^{-7}	3.20×10^{-5}	124.6413	2.400629
2	2222.723	1.00×10^{-7}	3.20×10^{-5}	125.0667	2.377873
3	4151.033	1.00×10^{-7}	3.20×10^{-5}	125.2414	2.369255
4	6446.303	1.00×10^{-7}	3.20×10^{-5}	125.3134	2.365821
5	9137.592	5.27×10^{-8}	3.20×10^{-5}	136.3971	2.273112
6	8873.021	4.28×10^{-8}	3.20×10^{-5}	140.8148	2.254192
7	10000	2.50×10^{-8}	3.20×10^{-5}	154.6842	2.219387
8	9122.437	2.05×10^{-8}	3.20×10^{-5}	160.7198	2.211236
9	9577.98	1.23×10^{-8}	3.20×10^{-5}	179.3340	2.195483
10	9994.321	1.09×10^{-8}	3.20×10^{-5}	184.8145	2.192491

and polynomial mutation operator [34], respectively. These two operators are used to deal with the upper and lower bound. The settings for NSGA-II controllable parameters would be strongly affected the responses. The authors have many experiences using the Taguchi experimental method to set parameters to improve system performances [35]–[37]. Therefore, in the study, the Taguchi method was used to arrange the settings for controllable parameters. The settings for NSGA-II were crossover rate = 0.9, mutation rate = 0.1, $\eta_c = 20$, and $\eta_m = 20$. Figure 8 shows the best solution space obtained. Table 2 shows the 10 sets of representative parameters chosen from 200 sets in the solution space.

B. MULTI-OBJECTIVE PARTICLE SWARM OPTIMIZATION (MOPSO)

The main architecture of the evolution process in this study was MOPSO, which was first proposed by Coello *et al.* [19]. This optimization method uses external temporary data to

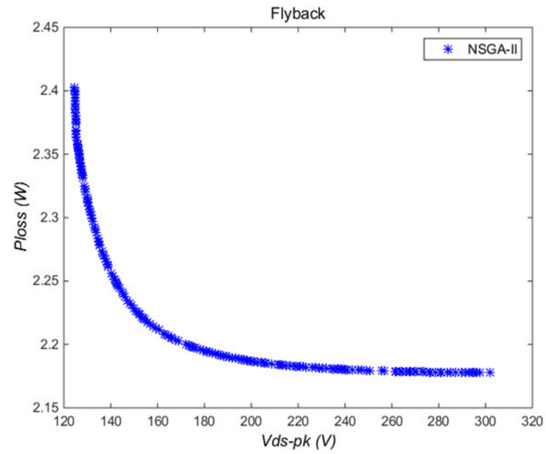

FIGURE 8. Non-dominated solution set obtained by NSGA-II.

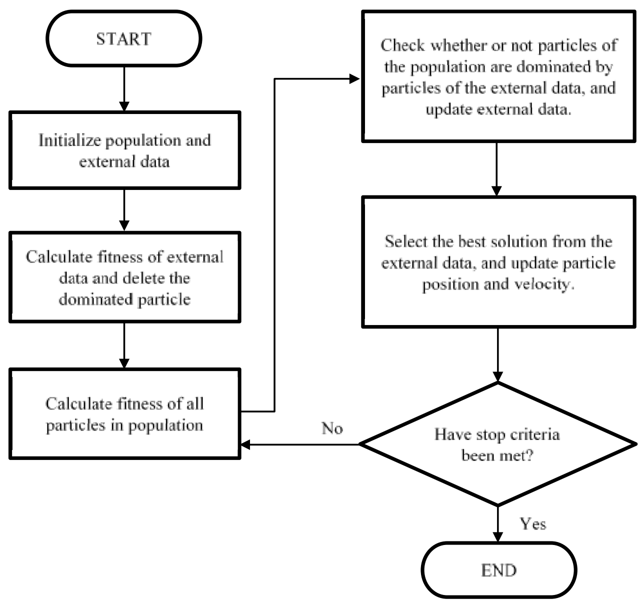

FIGURE 9. Flowchart of multi-objective particle swarm optimization.

retain the non-dominated solution set in each iteration. The particles are then guided to the best solution by the non-dominated solution in the external temporary data. This optimization method increases the capability to search for the best solution. Figure 9 is a flow chart of the MOPSO used in this study.

In MOPSO, c_1, c_2, and χ are set to 2.05, 2.05, and 0.73, respectively, obtained by the Taguchi method. Figure 10 shows the best solution space obtained by MOPSO. Table 3 shows the ten representative parameter sets chosen from the 200 parameter sets in the solution space.

C. MULTI-OBJECTIVE DIFFERENTIAL EVOLUTION ALGORITHM (MODE)

Many different methods of applying MODE have been proposed in recent years [21]. This study used the MODE

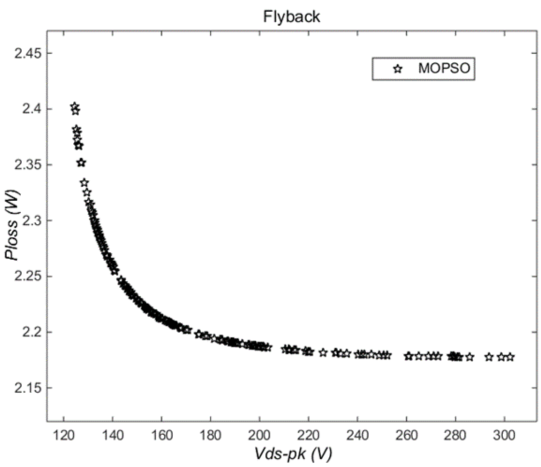

FIGURE 10. Non-dominated solution set obtained by MOPSO.

TABLE 3. Parameters and values in MOPSO.

	R_s (Ω)	C_s (F)	L_e (H)	V_{ds_pk} (V)	P_{loss} (W)
1	3025.612	8.59×10^{-8}	3.20×10^{-5}	127.465	2.345774
2	6748.013	5.81×10^{-8}	3.20×10^{-5}	134.4513	2.284926
3	7101.365	3.97×10^{-8}	3.20×10^{-5}	142.5095	2.249287
4	8257.054	2.63×10^{-8}	3.20×10^{-5}	153.0747	2.222926
5	8644.814	1.94×10^{-8}	3.20×10^{-5}	162.5155	2.209384
6	9010	1.33×10^{-8}	3.20×10^{-5}	176.1308	2.197678
7	9168.822	9.79×10^{-9}	3.20×10^{-5}	189.5186	2.190886
8	9479.351	8.05×10^{-9}	3.20×10^{-5}	199.0917	2.187483
9	9537.169	7.40×10^{-9}	3.20×10^{-5}	203.4810	2.186263
10	10000	4.79×10^{-9}	3.20×10^{-5}	229.5302	2.181344

TABLE 4. Parameters and values in MODE.

	R_s (Ω)	C_s (F)	L_e (H)	V_{ds_pk} (V)	P_{loss} (W)
1	2000	9.92×10^{-8}	3.20×10^{-5}	125.1435	2.378428
2	6400	7.39×10^{-8}	3.20×10^{-5}	130.0773	2.315755
3	8100	4.30×10^{-8}	3.20×10^{-5}	140.7024	2.25498
4	9400	2.34×10^{-8}	3.20×10^{-5}	156.6489	2.216572
5	7500	1.61×10^{-8}	3.20×10^{-5}	168.9792	2.203846
6	8500	1.35×10^{-8}	3.20×10^{-5}	175.7426	2.198212
7	9100	1.07×10^{-8}	3.20×10^{-5}	185.5633	2.192586
8	7900	9.00×10^{-9}	3.20×10^{-5}	193.3868	2.190299
9	8700	8.67×10^{-9}	3.20×10^{-5}	195.2685	2.189109
10	9300	6.83×10^{-9}	3.20×10^{-5}	207.8702	2.185356

architecture proposed by Huang *et al.* as the main architecture of the evolutionary process [24]. Figure 11 is a flowchart showing how MODE applies the concept of external temporary data. The crossover rate of the MODE in this study was set to 0.6 and F was set to [0, 2], obtained by the Taguchi method. Figure 12 shows the best solution space obtained by MODE, and Table 4 shows the 10 representative parameter sets chosen from 200 sets in the solution space.

D. COMPARISON OF OPTIMIZATION METHODS

Figure 13 compares the performance of the three multi-objective optimization methods. Figure 13 shows that NSGA-II outperformed MODE and MOPSO. The MODE had the worst diversity. Since human judgement of optimization performance is unreliable, this study applied

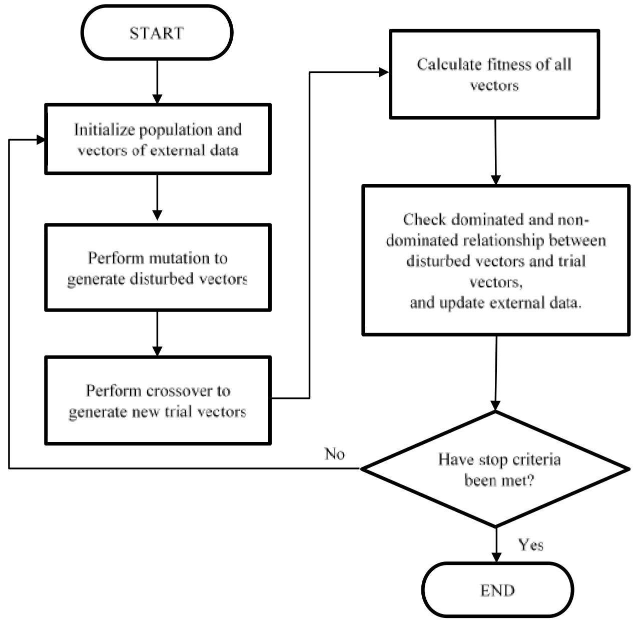

FIGURE 11. Flowchart of multi-objective differential evolution algorithm.

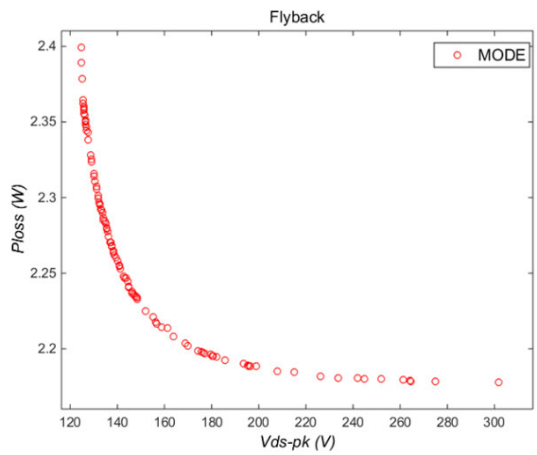

FIGURE 12. Non-dominated solution set obtained by MODE.

and discussed optimization performance evaluation methods described in the literature.

1) COVERAGE METRICS

For a clear performance comparison of different algorithms, the best non-dominated solutions obtained by multi-objective optimization were analyzed and compared. Here, coverage metrics (C) were calculated by two non-dominated solutions [38]. The calculation was the ratio of all solutions in non-dominated solution set V to all solutions dominated at U. The function was as follows:

$$C\ (U,V) = \frac{|\{b \in V | \exists a \in U, a \leq b\}|}{|V|}, \quad C \in [0,\ 1] \quad (3.1)$$

where $C\ (U,V) = 1$ means that all the non-dominated solution sets in V are dominated by U. Otherwise,

TABLE 5. Distance between non-dominated solutions and maximum dispersion distance.

Optimization	NSGA-II		MOPSO		MODE	
	S	*D*	*S*	*D*	*S*	*D*
1	0.001837	0.594562	0.00275067	0.594971453	0.013523	0.577267
2	0.001961	0.594561	0.00266272	0.589729396	0.005026	0.534491
3	0.001705	0.594557	0.003017626	0.593507701	0.006561	0.576389
4	0.001837	0.594562	0.003627334	0.591621091	0.015425	0.459076
5	0.002149	0.59456	0.00328783	0.585315864	0.005773	0.535424
6	0.001837	0.594562	0.00266272	0.589729396	0.009884	0.594443
7	0.001913	0.594566	0.003017626	0.593507701	0.017701	0.459325
8	0.001837	0.594562	0.002650913	0.592710142	0.008626	0.459188
9	0.00171	0.594604	0.003627334	0.591621091	0.005938	0.594067
10	0.00167	0.594552	0.00328783	0.585315864	0.007476	0.593629
Sum	0.018457	5.945649	0.030592602	5.9080297	0.095931	5.383298
Best	0.00167	0.5946	0.00265091	0.5949715	0.00503	0.59444
Mean	0.00185	0.59456	0.00305926	0.590803	0.00959	0.53833
Worst	0.00215	0.59455	0.00362733	0.5853159	0.0177	0.45908
Std.	0.000134	1.35×10-5	0.000364669	0.003154443	0.004227	0.055756
C.V.	7.256032	0.002269	11.92016456	0.533924726	44.06616	10.35726

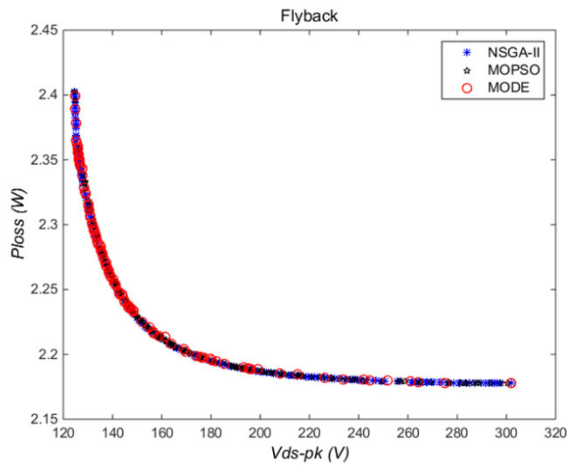

FIGURE 13. Performance comparison of three optimization methods.

$C(U, V) = 0$ means that all non-dominated solution sets in V are not dominated by U.

2) INTERVAL OF NON-DOMINATED SOLUTIONS (S)

The objective function values must be normalized before calculating the distance between the non-dominated solutions and the maximum dispersion distance. The distance between non-dominated solutions is calculated mainly to evaluate the distribution density of non-dominated solutions [39].

$$S = \sqrt{\frac{1}{N-1}\sum_{i=1}^{N}(d_i - \bar{d})^2} \tag{3.2}$$

$$d_i = \min \sum_{m=1}^{K} \left| f_m^i - f_m^j \right|, \quad i \neq j \tag{3.3}$$

where f_m is the objective function value of the non-dominated solution.

3) MAXIMUM DISPERSAL DISTANCE

The maximum dispersal distance (D) is defined as farthest distance between two non-dominated solutions in the set of non-dominated solutions. A large value for D indicates a wide distribution of optimization results. The calculation is as follows.

$$D = \sqrt{\sum_{m=1}^{K}(\max f_m^i - \min f_m^i)^2}, \quad i = 1, \ldots, N \tag{3.4}$$

To evaluate optimization performance, the interval between non-dominated solutions and the maximum dispersal distance is calculated for each of the three optimization methods. The coverage metrics between the optimizations is then calculated. For each of the three optimization methods, Table 5 shows the interval between the non-dominated solutions and the maximum dispersal distance. Table 6 further compares the coverage metrics between NSGA-II and MOPSO, between NSGA-II and MODE, and between MODE and MOPSO.

4) CONCLUSIONS OF PERFORMANCE EVALUATION

The experimental results in Tables V-VI show that each of the three multi-objective optimization methods revealed advantages and disadvantages. The average values obtained for the 10 representative parameter sets were used for the performance comparisons. The performance comparison results were as follows:

Coverage rate C (bigger the better):
NSGA-II > MODE > MOPSO.
Maximum dispersal distance D (bigger the better):
NSGA-II > MOPSO > MODE.
Non-dominated solution space S (smaller the better):
NSGA-II < MOPSO < MODE.

From above results and discussion, NSGA-II has better performance than MODE and MOPSO. Therefore, this paper used NSGA-II to optimize the design of an RCD buffer circuit.

E. TAGUCHI METHOD

The Taguchi method is a quality design method compiled and proposed by Taguchi [40]. Its main concept is to conduct

TABLE 6. Coverage metrics between optimizations.

Coverage Metrics	C(NSGA-II, MOPSO)	C(MOPSO, NSGA-II)	C(NSGA-II, MODE)	C(MODE, NSGA-II)	C(MOPSO, MODE)	C(MODE, OPSO)
1	0.575	0	0.315	0.015	0.18	0.585
2	0.63	0	0.275	0.015	0.11	0.57
3	0.31	0.005	0.235	0	0.16	0.22
4	0.395	0	0.28	0	0.11	0.36
5	0.62	0.005	0.35	0.04	0.135	0.61
6	0.565	0	0.39	0	0.245	0.49
7	0.335	0	0.27	0	0.09	0.145
8	0.515	0.015	0.235	0.015	0.145	0.445
9	0.445	0.005	0.315	0.025	0.14	0.465
10	0.57	0.01	0.46	0.01	0.19	0.59
Sum	4.96	0.04	3.125	0.12	1.505	4.48
Best	0.63	0.015	0.46	0.04	0.245	0.61
Mean	0.496	0.004	0.3125	0.012	0.1505	0.448
Worst	0.31	0	0.235	0	0.09	0.145
Std.	0.111126055	0.004898979	0.067426	0.01249	0.043327	0.152859

experimental design in a systematic way to understand the causes of product function variation in the most efficient way and try to find the ideal quality. The Taguchi method can effectively reduce experimental costs and obtain high-quality products. The use of orthogonal arrays for experimental planning is the most important step of the Taguchi method. Generally speaking, $L_a(b^c)$ is the symbol of the orthogonal array, a represents the number of experiments, b is the level number, and c is the number of factors that can be placed. Therefore, according to the needs, the appropriate orthogonal array can be selected for experimental configuration. Table 7 is a commonly used orthogonal array of $L_8(2^7)$. After the experiment configuration is completed and the experiment is executed, Table 8 is an example of $L_8(2^7)$. In Table 8, A_1 is the first level of factor A, A_2 is the second level of factor A, and the other factors and levels can be deduced by analogy; y is the experimental result, and η is the S/N ratio converted from the experimental result. Then, start to make a response table and draw a response chart. Table 9 and Figure 14 are examples of the response table and response chart, respectively. The response values of each level of each factor are averaged from the experimental results corresponding to the level. For example, the response value of A_1 in the response table is averaged from η_1, η_2, η_3, and η_4, as shown in Eq. (3.5).

$$A_1 = (\eta_1 + \eta_2 + \eta_3 + \eta_4) \div 4 \tag{3.5}$$

The response values of other factors and their levels are also calculated in the same way. The response chart is drawn from each response value in the response table. Finally, the best combination of factors can be obtained through the response table and response chart.

IV. OPTIMAL DESIGN OF RCD SNUBBER CIRCUIT

This study then used the NSGA-II to optimize the design of an RCD snubber circuit in a flyback converter. Figure 15 is a flowchart showing how the NSGA-II multi-objective optimization method searches within the wide range of the solution space and then converges the best non-dominated solutions in the best solution space. To obtain the optimal

TABLE 7. An orthogonal array of $L_8(2^7)$.

No. of experiments	Factors						
	A	B	C	D	E	F	G
1	1	1	1	1	1	1	1
2	1	1	1	2	2	2	2
3	1	2	2	1	1	2	2
4	1	2	2	2	2	1	1
5	2	1	2	1	2	1	2
6	2	1	2	2	1	2	1
7	2	2	1	1	2	2	1
8	2	2	1	2	1	1	2

TABLE 8. An example of $L_8(2^7)$ orthogonal array with Results.

No. of experiments	Factors							Results			S/N ratio
	A	B	C	D	E	F	G				
1	1	1	1	1	1	1	1	y_1^1	…	y_n^1	η_1
2	1	1	1	2	2	2	2	y_1^2	…	y_n^2	η_2
3	1	2	2	1	1	2	2	y_1^3	…	y_n^3	η_3
4	1	2	2	2	2	1	1	y_1^4	…	y_n^4	η_4
5	2	1	2	1	2	1	2	y_1^5	…	y_n^5	η_5
6	2	1	2	2	1	2	1	y_1^6	…	y_n^6	η_6
7	2	2	1	1	2	2	1	y_1^7	…	y_n^7	η_7
8	2	2	1	2	1	1	2	y_1^8	…	y_n^8	η_8

TABLE 9. A respond table of table 8.

Levels	Factors						
	A	B	C	D	E	F	G
1	A_1	B_1	C_1	D_1	E_1	F_1	G_1
2	A_2	B_2	C_2	D_2	E_2	F_2	G_2
Max-Min	a	b	c	d	e	f	g

design, the parameter combination most suitable for the user is then selected from the solution set and adjusted by the Taguchi method with actual passive components.

Although there are some softwares, like GAMS that is non-linear optimizer, the GAMS is a solver for single-objective problems. However, this study is a multiple-objective problem including both objectives of V_{ds} and P_{loss}. The classical algorithms for multi-objective problems include NSGA-II, MOPSO, and MODE. Therefore, this study used the three algorithms to solve the RCD buffer circuit problem and

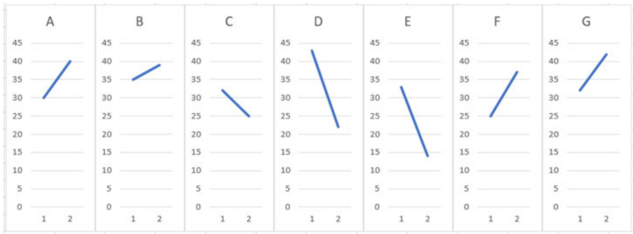

FIGURE 14. An Example of response chart.

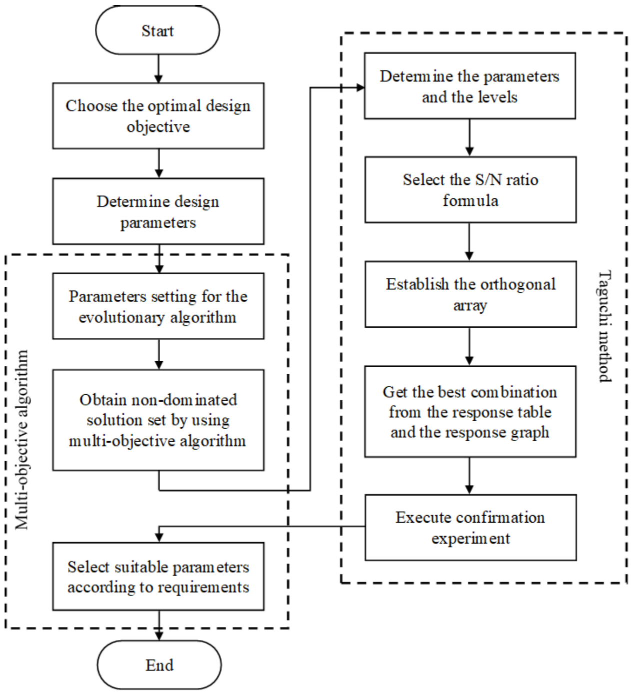

FIGURE 15. Flowchart of multi-objective optimization for circuit design.

TABLE 10. Parameters obtained by NSGA-II and previous design.

Optimization	$R_s(K\Omega)$	$C_s(nF)$	$L_e(\mu H)$
NSGA-II (Trade-off)	9.1194	21.42	32
Previous design	10	10	43.5

compared them in term of performance. From the results, NSGA-II has better performance among the three algorithms.

Comparisons of the three algorithms confirmed the superior performance of the NSGA-II. Therefore, NSGA-II was then used to find the optimal solution space. Since multi-objective optimization obtains elastic sets of solutions instead of a single optimal solution, users can choose suitable solutions from the solution set according to their needs. Since the two objectives in this experiment had equal importance, the trade-off parameters were selected as the snubber parameters of the flyback converter. Table 10 shows a set of parameters obtained by NSGA-II and previous design. Figure 16 shows the optimization results.

The results in Table 10 are continuous theoretical values. In a real-world application, components with these best-case parameters would probably be unavailable. Therefore, the orthogonal experiment in this study was performed using the actual values for three commercially available models

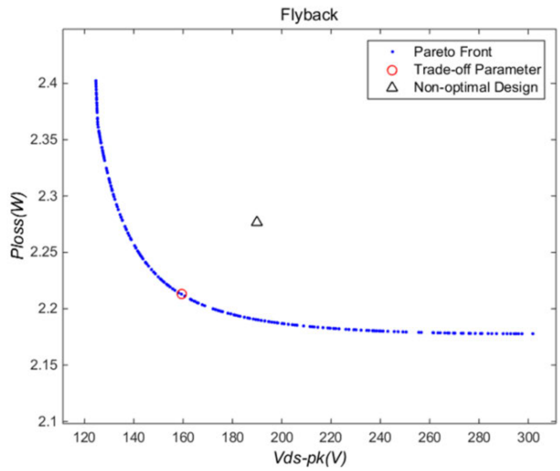

FIGURE 16. Comparison of results obtained by Trade-off and previous design parameters.

TABLE 11. Parameters obtained by NSGA-II and previous design.

Control parameters	Description	Level 1	Level 2	Level 3
A	Resistance $(K\Omega)$	8.2	9.1	10
B	Clamp Capacitor (nF)	18	22	27
C	Leakage Inductor (μH)	32	43.5	58

TABLE 12. The $L_9(3^4)$ orthogonal array and experimental values.

No.	*A*	*B*	*C*	V_{ds_pk}	P_{loss}	*Y*	MSD	S/N
1	1	1	1	0.8854	0.9112	1.2706	1.6143	-2.0799
2	1	2	2	0.9271	0.9501	1.3275	1.7621	-2.4604
3	1	3	3	0.9167	1	1.3566	1.8403	-2.6488
4	2	1	2	0.9375	0.9467	1.3323	1.7751	-2.4921
5	2	2	3	0.9583	0.9958	1.3820	1.9100	-2.8103
6	2	3	1	0.875	0.9181	1.2683	1.6086	-2.0644
7	3	1	3	1	0.9924	1.4089	1.9849	-2.9773
8	3	2	1	0.8958	0.9140	1.2798	1.6379	-2.1423
9	3	3	2	0.9479	0.9538	1.3447	1.8082	-2.5725

to approximate the theoretical values obtained by NSGA-II. Table 11 shows the control factors and levels.

Since the three-factor experiment with three levels requires 6 degrees of freedom, the orthogonal array selects $L_9(3^4)$. In this case, the S/N ratio of the smaller the better was adopted. The V_{ds} and P_{loss} were obtained by direct measurement. To prevent the use of different units from affecting the results, data for the two objectives were normalized before the experiment was executed. Table 12 shows the orthogonal array and data.

Table 13 and Figure 17 are the response table and chart, respectively, obtained according to the S/N ratios in each experiment. The data in the table and figure show that the best parameter combination in the experiments was $A_1B_3C_1$.

Finally, a validation experiment was performed using the best parameter combination. Table 14 shows the trade-off best results, obtained by the NSGA-II, MOPSO, and MODE, and the optimal results, achieved from the method obtained by NSGA-II and tuned by the Taguchi (NSGA-II-Taguchi) method, and comparison with the previous design method. Figure 18 shows the actual circuit with the

TABLE 13. Response table from orthogonal array and experimental values.

	A	B	C
Level 1	-2.396364	-2.51643	-2.09572
Level 2	-2.455631	-2.47121	-2.50834
Level 3	-2.564221	-2.42857	-2.81216
Max-Min	0.167857	0.087859	0.716433

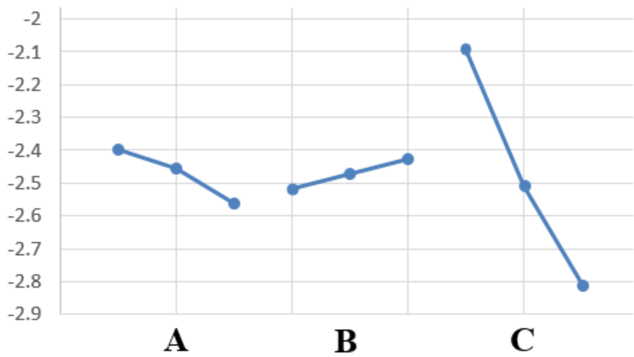

FIGURE 17. Response chart according to results in response table.

TABLE 14. Comparison of trade-off parameter and result obtained by different methods (considered two objectives).

Methods	Parameters			Outputs		Reduction percentages	
	$R_s(K\Omega)$	$C_s(nF)$	$L_e(\mu H)$	$V_{ds}(V)$	$P_{loss}(W)$	V_{ds} (%)	$P_{loss}(W)$
NSGA-II-Taguchi method	8.2	27	32	162	2.2242	14.74%	2.31%
NSGA-II (Trade-off)	9.1	22	32	164	2.2342	13.68%	1.87%
MOPSO (Trade-off)	8.9	25	32	168	2.2402	11.58%	1.60%
MODE (Trade-off)	9.2	23	32	165	2.2592	13.16%	0.77%
Previous design	10	10	43.5	190	2.2767	-	-

optimized parameters. Figure 19 shows the V_{ds} waveform with $V_{dsp} = 162V$. A comparison with the waveform before optimization (Figure 20 with $V_{dsp} = 190V$) reveals a substantial improvement. Reduction percentages, compared with the previous design result, for V_{ds} and P_{loss} by the NSGA-II-Taguchi method are 14.74% and 2.31%, respectively. Reduction percentages, compared with the previous design result, for V_{ds} obtained by the NSGA-II, MOPSO, and MODE are 13.68%, 11.58%, and 13.16%, and for P_{loss} obtained by the NSGA-II, MOPSO, and MODE are 1.87%, 1.60%, and 0.77%, respectively. From Table 14, the trade-off best result obtained the NSGA-II-Taguchi method has better performance.

Huang *et al.* [5], [6] used a GA-related algorithm and the Taguchi method to optimize the design of DC-DC converter for spike voltage reduction. In this paper, the authors attempt to just consider the influence of peak voltage. For comparing performances between the NSGA-II-Taguchi method and the method of Huang *et al.* [5], [6], the V_{ds} is regarded as the objective. The V_{ds} can be obtained $125V$

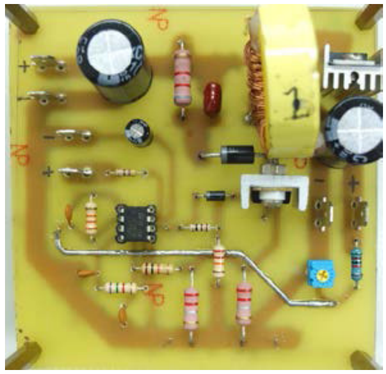

FIGURE 18. Circuit fabricated with optimized parameters.

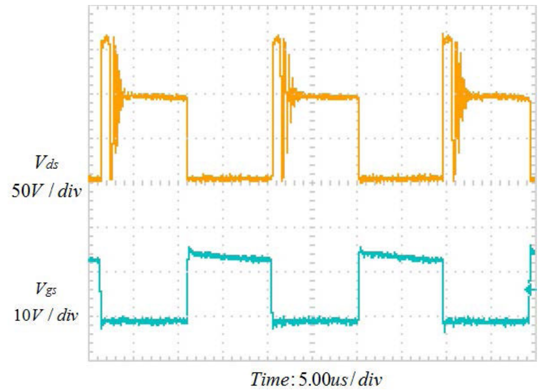

FIGURE 19. The V_{da} waveform for circuit fabricated with optimized parameters (V_{dsp} = 162V).

TABLE 15. Comparison of parameter and result obtained by different methods (only considered V_{ds}).

Method	Parameters			Output	Reduction percentage
	$R_s(K\Omega)$	$C_s(nF)$	$L_e(\mu H)$	$V_{ds}(V)$	V_{ds} (%)
NSGA-II-Taguchi method	1	100	32	125	34.21%
Huang et al. (2008, 2010)	15	150	1.08	138	27.37%
Previous design	10	10	43.5	190	-

with $R_s = 1\ k\Omega$, $C_s = 100\ nF$, and $L_e = 32\ \mu H$ by the NSGA-II-Taguchi method. Table 15 shows the experimental results obtained by the NSGA-II-Taguchi method and the method of Huang *et al.* [5], [6] and comparison with the previous design method. Figure 21 shows the V_{ds} waveform with $V_{dsp} = 125V$, and it also indicates a more substantial improvement by contrast with Figure 20. The optimized result is also better than that with $V_{dsp} = 138V$ obtained by the method of Huang *et al.* [5], [6]. Reduction percentage, compared with the previous design result, for V_{ds} obtained by the method Huang *et al.* [5], [6] is 27.37% and for V_{ds} obtained by the NOTT is 34.21%. Therefore, the optimal method obtained by the NSGA-II-Taguchi method for designing a DC-DC converter with an RCD snubber is effective and feasible.

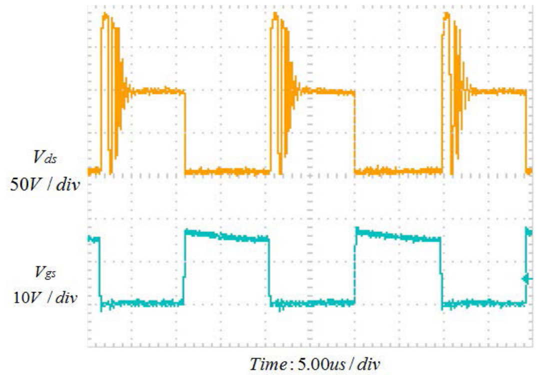

FIGURE 20. The V_{ds} waveform for circuit fabricated without optimized parameters (V_{dsp} = 190V).

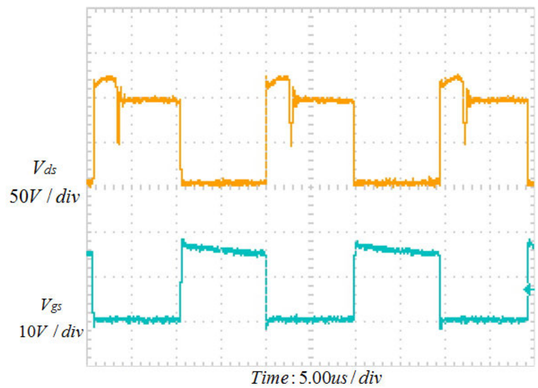

FIGURE 21. The V_{ds} waveform for circuit fabricated with optimized parameters (V_{dsp} = 125V).

V. CONCLUSION

This study used NSGA-II and Taguchi method to optimize the parameter values for an RCD snubber circuit of a DC-DC flyback converter. The above discussion of the working principle of the RCD snubber circuit in the flyback converter described the circuit components that affect the power switch voltage loss and circuit energy loss, which were used as parameters. Three multi-objective optimization methods were implemented and analyzed: NSGA-II, MOPSO, and MODE. Comparisons confirmed the superior performance of NSGA-II. Additionally, the specific steps needed to implement a practical design after the optimal solution space is calculated by the NSGA-II algorithm. By combining NSGA-II algorithm with Taguchi method, the proposed method can obtain the optimal design without the need for practical experience or trial-and-error method. At the same time, the proposed method solves the problem of theoretical optimization results being restricted by the currently existing component specifications. The design results were realized in the fabrication of a printed circuit board. The experiment verified that performance with the proposed parameter optimization is superior to those without parameter optimization as well as with parameter optimization given by Huang *et al.* [5], [6]. Notably, the process required only nine experiments, which substantially reduced circuit design time and cost. For application in industries, the proposed NSGA-II-Taguchi method can quickly find design parameters and reduce the complexity of considering both spike voltage and energy loss on the RCD snubber circuit. From the real applied responses of Metal Industries Research and Development Centre (www.mirdc.org.tw) and cooperation manufacturers, it has been approved that the RCD snubber circuit designed by the proposed NSGA-II-Taguchi method can improve the effectiveness of the equipment in reducing spike voltage and energy loss. Thus, the proposed optimization method is both economical and practical.

REFERENCES

[1] F. Zhu, F. Liu, W. Liu, K. Feng, and X. Zha, "Performance analysis of RCD and MOV snubber circuits in low-voltage DC microgrid system," in *Proc. IEEE Appl. Power Electron. Conf. Expo. (APEC)*, Mar. 2017, pp. 1518–1521.

[2] Y. Yamashita, J. Furuta, S. Inamori, and K. Kobayashi, "Design of RCD snubber considering wiring inductance for MHz-switching of SiC-MOSFET," in *Proc. IEEE 18th Workshop Control Modeling Power Electron. (COMPEL)*, Jul. 2017, pp. 1–6, doi: 10.1109/COMPEL.2017.8013396.

[3] R. Parvari, M. Zarghani, and S. Kaboli, "RCD snubber design based on reliability consideration: A case study for thermal balancing in power electronic converters," *Microelectron. Rel.*, vols. 88–90, pp. 1311–1315, Sep. 2018, doi: 10.1016/j.microrel.2018.06.072.

[4] X. Sun, H. Long, D. Liu, and P. Li, "Multi-objective optimization design for snubber in switching power amplifier," in *Proc. Int. Conf. Electr. Mach. Syst.*, Tokyo, Japan, Nov. 2009, pp. 1–6.

[5] C. K. Huang, H. H. Nien, K. Y. Chang, and W. J. Chang, "An optimal designed RCD snubber for DC-DC converters," *J. Mar. Sci. Technol.*, vol. 18, no. 6, pp. 901–906, 2010.

[6] C. K. Huang, H. H. Nien, S. K. Changchien, C. H. Chan, and C. K. Chen, "An optimal designed RCD snubber for DC-DC converters," in *Proc. 10th Int. Conf. Control, Autom., Robot. Vis.*, Dec. 2008, pp. 2202–2207.

[7] D. V. Malyna, J. L. Duarte, M. A. M. Hendrix, and F. B. M. van Horck, "Multi-objective optimization of power converters using genetic algorithms," in *Proc. Int. Symp. Power Electron., Electr. Drives, Autom. Motion (SPEEDAM)*, 2006, pp. 713–717.

[8] C. Versele, O. Deblecker, and J. Lobry, "Multiobjective optimal design of transformers for isolated switch mode power supplies," in *Proc. SPEEDAM*, Jun. 2010, pp. 1687–1692.

[9] C. Versèle, O. Deblecker, and J. Lobry, "A computer-aided design tool dedicated to isolated DC-DC converters based on multiobjective optimization using genetic algorithms," *COMPEL Int. J. Comput. Math. Electr. Electron. Eng.*, vol. 31, no. 2, pp. 583–603, Mar. 2012.

[10] P. Lefranc, X. Jannot, and P. Dessante, "Virtual prototyping and pre-sizing methodology for buck DC-DC converters using genetic algorithms," *IET Power Electron.*, vol. 5, no. 1, pp. 41–52, Jan. 2012.

[11] J. D. Schaffer, "Multiple objective optimization with vector evaluated genetic algorithms," in *Proc. 1st Int. Conf. Genetic Algorithms*, 1985, pp. 93–100.

[12] P. Hajela and C.-Y. Lin, "Genetic search strategies in multicriterion optimal design," *Struct. Optim.*, vol. 4, no. 2, pp. 99–107, Jun. 1992.

[13] C. M. Fonseca, and P. J. Fleming, "Genetic algorithms for multiobjective optimization: Formulation discussion and generalization," in *Proc. 5th Int. Conf. Genetic Algorithms*, vol. 423, 1993, pp. 416–423.

[14] K. Deb, and N. Srinivas, "Multi-objective optimization using nondominated sorting in genetic algorithms," *Evol. Comput.*, vol. 2, no. 3, pp. 221–248, 1994.

[15] K. Deb, A. Pratap, S. Agarwal, and T. Meyarivan, "A fast and elitist multiobjective genetic algorithm: NSGA-II," *IEEE Trans. Evol. Comput.*, vol. 6, no. 2, pp. 182–197, Apr. 2002.

[16] Q. Liu and G. Jiao, "A pipe routing method considering vibration for aero-engine using kriging model and NSGA-II," *IEEE Access*, vol. 6, pp. 6286–6292, 2018.

[17] C. Wan, M. Niu, Y. Song, and Z. Xu, "Pareto optimal prediction intervals of electricity price," *IEEE Trans. Power Syst.*, vol. 32, no. 1, pp. 817–819, Jan. 2017.

[18] C. A. C. Coello, and M. S. Lechuga, "A proposal for multiple objective particle swarm," in *Proc. Congr.*, vol. 2, 2002, pp. 1051–1056.
[19] C. A. C. Coello, G. T. Pulido, and M. S. Lechuga, "Handling multiple objectives with particle swarm optimization," *IEEE Trans. Evol. Comput.*, vol. 8, no. 3, pp. 256–279, Jun. 2004.
[20] T. Kumrai, K. Ota, M. Dong, J. Kishigami, and D. K. Sung, "Multi-objective optimization in cloud brokering systems for connected Internet of Things," *IEEE Internet Things J.*, vol. 4, no. 2, pp. 404–413, Apr. 2017.
[21] H. A. Abbass, R. Sarker, and C. Newton, "PDE: A Pareto-frontier differential evolution approach for multi-objective optimization problems," in *Proc. Congr. Evol. Comput.*, vol. 2, 2001, pp. 971–978.
[22] B. V. Babu, and M. M. L. Jehan, "Differential evolution for multi-objective optimization," in *Proc. Congr. Evol. Comput.*, vol. 4, Dec. 2003, pp. 2696–2703.
[23] S. Kukkonen and J. Lampinen, "GDE3: The third evolution step of generalized differential evolution," in *Proc. IEEE Congr. Evol. Comput.*, vol. 1, 2005, pp. 443–450.
[24] V. L. Huang, A. K. Qin, P. N. Suganthan, and M. F. Tasgetiren, "Multi-objective optimization based on self-adaptive differential evolution algorithm," in *Proc. IEEE Congr. Evol. Comput.*, Sep. 2007, pp. 3601–3608.
[25] S. Mirjalili, "Dragonfly algorithm: A new meta-heuristic optimization technique for solving single-objective, discrete, and multi-objective problems," *Neural Comput. Appl.*, vol. 27, no. 4, pp. 1053–1073, May 2016.
[26] Y. Shen and Y. Wang, "Operating point optimization of auxiliary power unit using adaptive multi-objective differential evolution algorithm," *IEEE Trans. Ind. Electron.*, vol. 64, no. 1, pp. 115–124, Jan. 2017.
[27] N. Le Chau, V. A. Dang, H. G. Le, and T.-P. Dao, "Robust parameter design and analysis of a leaf compliant joint for micropositioning systems," *Arabian J. Sci. Eng.*, vol. 42, no. 11, pp. 4811–4823, Nov. 2017.
[28] T. P. Dao, and S. C. Huang, "Design and multi-objective optimization for a broad self-amplified 2-DOF monolithic mechanism," *Sādhanā*, vol. 42, no. 9, pp. 1–16, 2017.
[29] T.-P. Dao, S.-C. Huang, and P. T. Thang, "Hybrid taguchi-cuckoo search algorithm for optimization of a compliant focus positioning platform," *Appl. Soft Comput.*, vol. 57, pp. 526–538, Aug. 2017.
[30] S.-C. Huang and T.-P. Dao, "Multi-objective optimal design of a 2-DOF flexure-based mechanism using hybrid approach of grey-taguchi coupled response surface methodology and entropy measurement," *Arabian J. Sci. Eng.*, vol. 41, no. 12, pp. 5215–5231, Dec. 2016.
[31] N.-T. Huynh, S.-C. Huang, and T.-P. Dao, "Optimal displacement amplification ratio of bridge-type compliant mechanism flexure hinge using the Taguchi method with grey relational analysis," *Microsyst. Technol.*, pp. 1–15, Oct. 2018.
[32] A. Hren, J. Korelic, and M. Milanovic, "RC-RCD clamp circuit for ringing losses reduction in a flyback converter," *IEEE Trans. Circuits Syst. II, Exp. Briefs*, vol. 53, no. 5, pp. 369–373, May 2006.
[33] K. Deb and R. B. Agrawal, "Simulated binary crossover for continuous search space," *Complex Syst.*, vol. 9, no. 2, pp. 115–148, 1995.
[34] M. M. Raghuwanshi, and O. G. Kakde, "Survey on multiobjective evolutionary and real coded genetic algorithms," in *Proc. 8th Asia Pacific Symp. Intell. Evol. Syst.*, 2004, pp. 150–161.
[35] C. C. Chiu, F. I. Chou, M. Y. Cheng, and J. T. Tsai, "Optimization of process parameters for gilding stamping by Taguchi and image processing methods," *J. Chin. Soc. Mech. Eng.*, vol. 37, no. 1, pp. 21–29, 2016.
[36] J.-T. Tsai, C.-C. Chang, W.-P. Chen, and J.-H. Chou, "Optimal parameter design for IC wire bonding process by using fuzzy logic and Taguchi method," *IEEE Access*, vol. 4, pp. 3034–3045, 2016.
[37] J.-T. Tsai, C.-T. Lin, and J.-H. Chou, "Intelligent data-driven adaptive method for optimizing system integration scaling factors for touch panel lamination machines," *IEEE Trans. Syst., Man, Cybern. Syst.*, vol. 50, no. 4, pp. 1300–1309, Apr. 2020, doi: 10.1109/TSMC.2017.2707441.
[38] T. Okabe, Y. Jin, and B. Sendhoff, "A critical survey of performance indices for multi-objective optimisation," in *Proc. Congr. Evol. Comput. (CEC)*, vol. 2, Dec. 2003, pp. 878–885.
[39] J. R. Schott, "Fault tolerant design using single and multi-criteria genetic algorithm optimization," M.S. thesis, Dept. Aeronaut. Astronaut., Massachusetts Inst. Technol., Cambridge, MA, USA, 1995.
[40] G. Taguchi, *Systems of Experimental Design*. White Plains, NY, USA: Unipub/Kraus International Publications, 1987.

YING MA received the B.S. degree in electrical engineering and automation from Fuzhou University, Fujian, China, in 2002, and the M.S. degree in information science and engineering from Central South University, Hunan, China, in 2008.

She is currently an Associate Professor with the School of Information Science and Engineering, Fujian University of Technology, Fujian. Her research interests include computational intelligence, evolutionary computation, neural networks, and integration technology of automation systems.

FU-I CHOU received the B.S. degree in electrical engineering from the National University of Kaohsiung, Taiwan, in 2010, the M.S. degree in electrical engineering from National Dong-Hwa University, Taiwan, in 2012, and the Ph.D. degree in electrical engineering from National Cheng-Kung University, Taiwan, in 2019. From August 2019 to January 2020, he was an Assistant Professor with the National Chin-Yi University of Technology, Taiwan. He was a Deputy Engineer with the Metal Industries Research and Development Centre, Taiwan, from September 2012 to August 2019. He is currently an Assistant Professor with the Department of Automation Engineering, National Formosa University, Taiwan. His research interests include state observer design, automation and control, industrial robotics, artificial intelligence applications, machine learning, quality engineering, evolutionary optimization, and machine vision. He received the 2019 Doctoral Dissertation Award from the Chinese Automatic Control Society, Taiwan. He and his colleagues proposed the research and development achievement, Intelligent 3D Visual Automation for Shoes Roughing and Cementing Equipment, received the 2019 American Edison Bronze Award in robot field, and the Sixth National Industry Innovation Award from the Taiwan Ministry of Economics.

PO-YUAN YANG received the B.S. and M.S. degrees in computer science from National Pingtung University, Pingtung, Taiwan, in 2011 and 2014, respectively, and the Ph.D. degree in electrical engineering from the National Kaohsiung University of Science and Technology, Kaohsiung, Taiwan, in 2019.

From March 2019 to January 2020, he was a Postdoctoral Researcher with the Department of Electrical Engineering, National Kaohsiung University of Science and Technology. He is currently an Assistant Professor with the Department of Information Engineering and Computer Science, Feng Chia University, Taichung, Taiwan. His research interests include evolutionary algorithms, image processing, neural networks, data analysis, and quality engineering.

JINN-TSONG TSAI received the B.S. and M.S. degrees in mechanical and electro-mechanical engineering from National Sun Yat-sen University, Taiwan, in 1986 and 1988, respectively, and the Ph.D. degree in engineering science and technology from the National Kaohsiung University of Science and Technology, Taiwan, in 2004.

From July 1988 to May 1990, he was a Lecturer with the Vehicle Engineering Department, Chung Cheng Institute of Technology, Taiwan. From July 1990 to August 2004, he was a Researcher and the Chief of the Automation Control Section, Metal Industries Research and Development Center, Taiwan. From September 2004 to July 2006, he was an Assistant Professor with the Medical Information Management Department, Kaohsiung Medical University, Kaohsiung, Taiwan. From August 2006 to July 2010, he was an Assistant Professor, from August 2010 to January 2014, he was an Associate Professor, and from February 2014 to July 2018, he was a Professor with the Department of Computer Science, National Pingtung University, Pingtung, Taiwan, where he is currently a Distinguished Professor. His research interests include computational intelligence, machine learning, robust optimization, and intelligent control and systems.

ZHEN-YU YANG received the B.S. degree in aeronautical engineering from National Formosa University, Yunlin, Taiwan, in 2010, and the M.S. degree in system information and control from the National Kaohsiung University of Science and Technology, Kaohsiung, Taiwan, in 2012.

He is currently an Electrical/Control System Engineer with Kenmec Mechanical Engineering Company Ltd., Taiwan.

JYH-HORNG CHOU (Fellow, IEEE) received the B.S. and M.S. degrees in engineering science from National Cheng-Kung University, Tainan, Taiwan, in 1981 and 1983, respectively, and the Ph.D. degree in mechatronic engineering from National Sun Yat-sen University, Kaohsiung, Taiwan, in 1988. He is currently a Chair Professor with the Electrical Engineering Department, National Kaohsiung University of Science and Technology, Taiwan. He has coauthored four books and published over 265 refereed journal articles. He holds six patents. His research and teaching interests include intelligent systems and control, computational intelligence and methods, automation technology, robust control, and robust optimization. He is a Fellow of the Institution of Engineering and Technology (IET), the Chinese Automatic Control Society (CACS), the Chinese Institute of Automation Engineer (CIAE), and the Chinese Society of Mechanical Engineers (CSME). He was a recipient of the 2011 Distinguished Research Award from the National Science Council of Taiwan, the 2012 IEEE Outstanding Technical Achievement Award from the IEEE Tainan Section, the 2014 Distinguished Research Award from the Ministry of Science and Technology of Taiwan, the Research Award and the Excellent Research Award from the National Science Council of Taiwan 14 times, and numerous academic awards/honors from various Societies. In the IEEE Computational Intelligence Society (IEEE CIS) Evaluation, Industrial Application Success Story, received the 2014 Winner of highest rank, selected to become the first internationally industrial success story being reported on the IEEE CIS website.